Supplementary figures

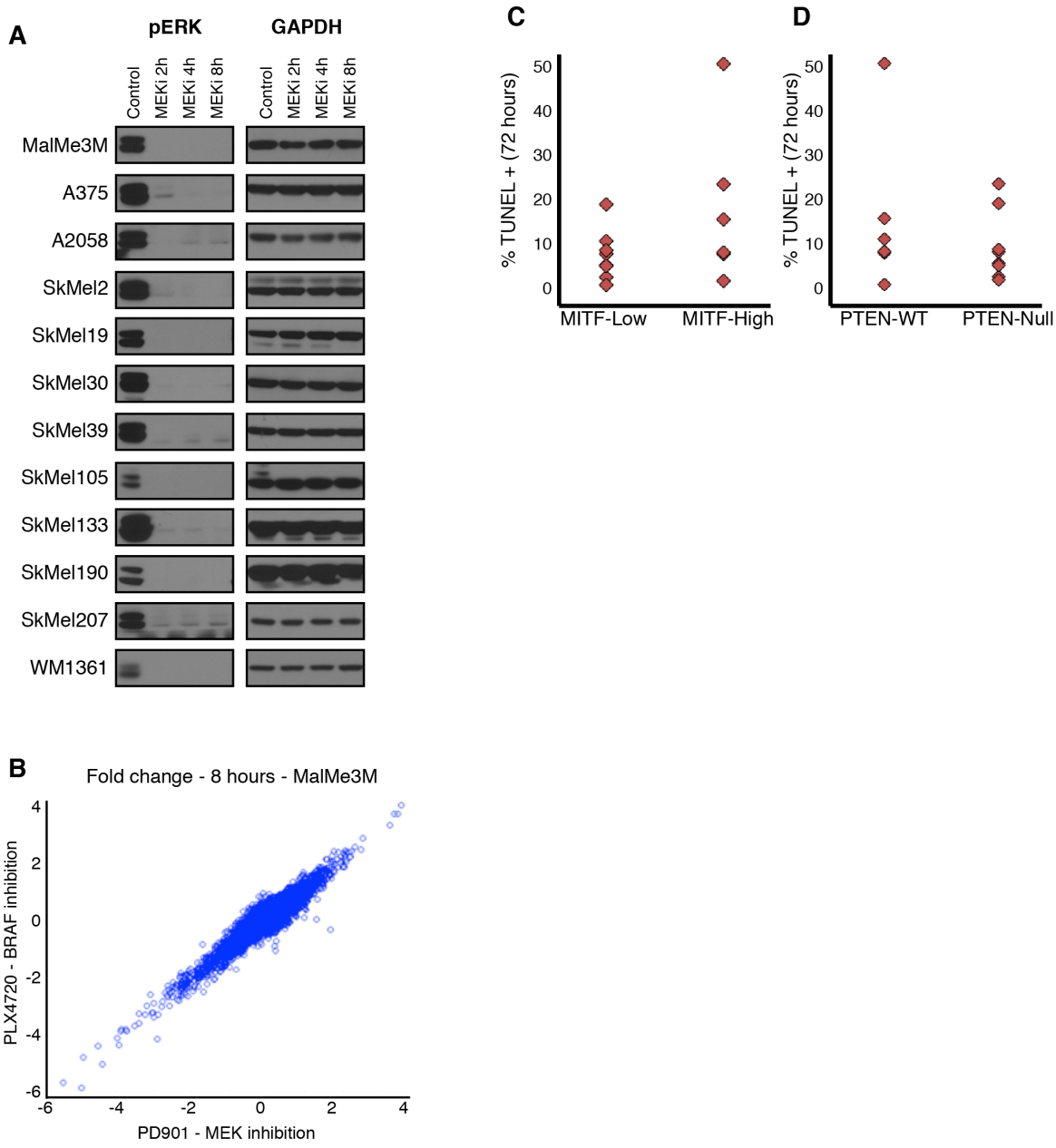

Figure S1 – Related to Figure 1 – Response to MAPK inhibition **A.** pERK levels in all cell lines, 2, 4 and 8 hours following treatment with PD901. pERK stays low throughput the 8 hours and therefore does not explain the heterogeneity observed between cell lines. **B.** Comparison of MEK and BRAF inhibitors in a BRAF-V600E cell line shows an almost identical transcriptional response. Scatter plot shows fold change of all genes

with a 50nM of PD325901, a MEK inhibitor (x-axis), compared with a 2uM of PLX4720, a BRAF inhibitor (y-axis). Almost all genes fall directly on the diagonal. Colo829 doesn't grow in the conditions used to generate these growth curves. **C-D**. Scatter plots representation of the data in figure 1B. Each dot represents the difference of percentage of TUNEL+ cells between PD901 and DMSO, dividing MITF+ and MITF- cell lines (B), and PTEN-WT and PTEN-null (C). These mutations do not fully explain the phenotypic differences between cell lines.

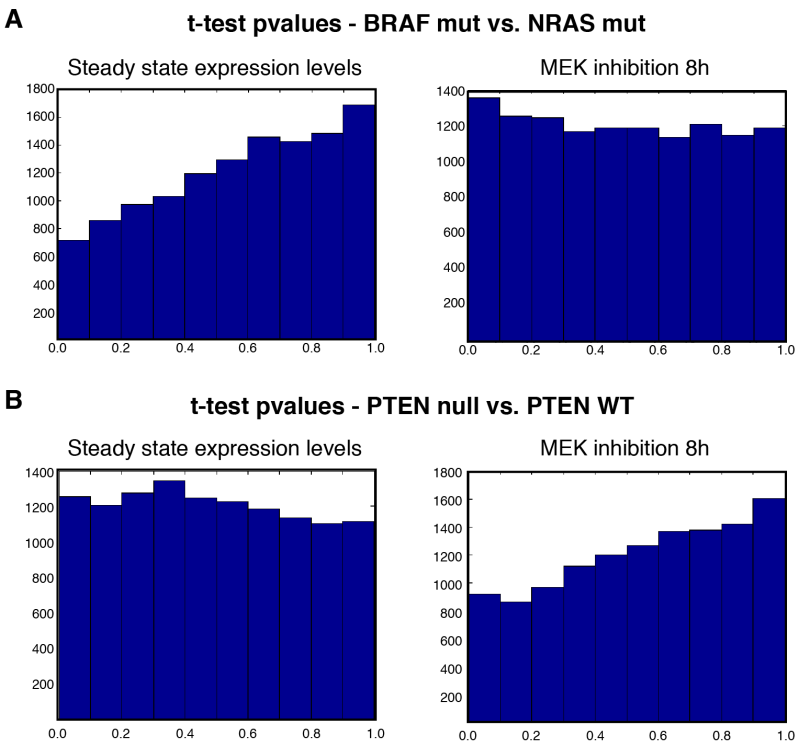

Figure S2 – Related to figure 2 – Correlation between known genetic variants and gene expression - **A.** Histograms of p-values comparing expression levels of BRAF-mut with NRAS-mut cell lines using t-test, before and after pathway inhibition. No gene passes FDR correction with q-value<0.05. See number of targeted genes in figure 2. **B.** Histograms of p-values comparing expression levels of PTEN-null/mut with PTEN-WT in BRAF-mut cell lines using t-test, before and after pathway inhibition. No gene passes FDR correction with qvalue<0.05.

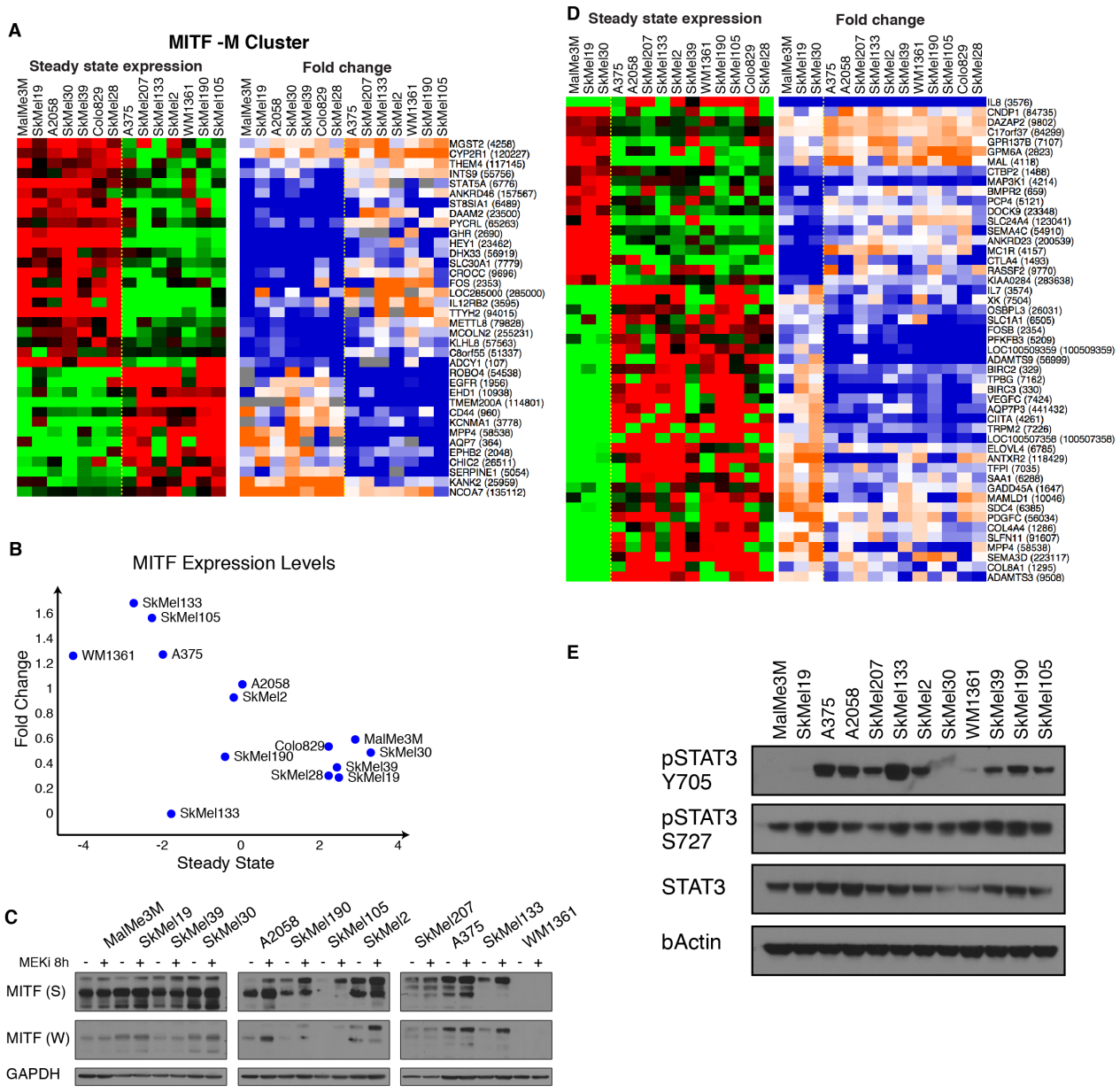

Figure S3 – Related to figure 4 – COSPER links pathway activity with gene expression levels - **A.** Full cluster, including all genes, of the cluster presented in figure 3A. **B.** MITF mRNA expression levels before (x-axis) and after (y-axis) MEK inhibition. Steady state and fold change levels are negatively correlated. **C.** Levels of MITF protein isoforms in 12 cell lines, before and 8 hours after MEK inhibition. Each isoform is regulated to different degrees in the different cell lines, supporting a context-specific control of MITF by the MAPK pathway.. Strong (S) and Weak (W) film exposures are shown. **D.** COSPER clusters together genes with the same context-specific regulation but with different regulation patterns. For example, the cluster here is associated with the STAT3

context, but contains 3 regulation patterns. The cluster in figure 4C shows one such pattern out of the 3 identified by COSPER. **E.** Levels of STAT3 and pSTAT3-S727 are similar in all cell lines and do not explain the differential activation of pSTAT3-Y705.

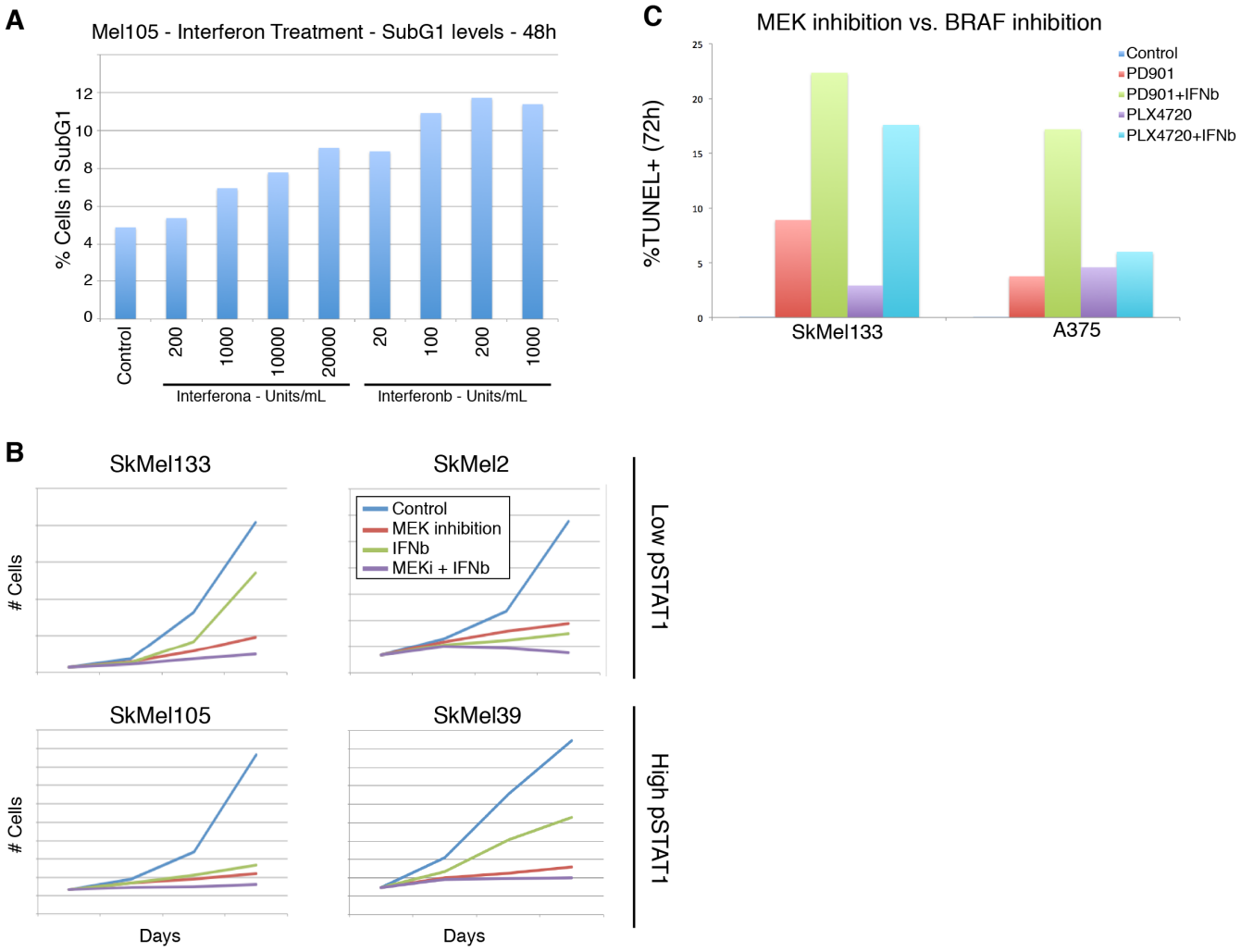

Figure S4 – Related to figure 5 – Response to IFNα/β treatment - **A.** Dose-dependent response to IFNα and β. The cytotoxicity of IFN was assessed in high pSTAT1 cell line, 48 hours after treatment using SubG1 percentage. IFNα has a weaker cytotoxic effect than IFNβ, and both show dose-dependent effects. 1000Units/mL of IFNβ was used for all experiments in this manuscript. Cells plated in 6 well plates, 200K cells/well, in 2mL of growth media. **B.** Growth curves of 2 low- (top) and 2 high- (bottom) pSTAT1 cell lines with MEK inhibition, IFNβ or both. 50K cells per well were plated in 6-well plates with 2mL of media and treated 24 hours later. Cells were counted every 24 hours up to 72 hours. Cytotoxic levels in figure 5E. **C.** Comparison of MEK inhibition and BRAF inhibition, with and without combination with IFNβ. Cells were plated in 6 well plates, 200K cells/well with 2mL media. 24 hours after plating cells were treated with DMSO, 50nM PD901 with or without IFNβ, 2uL of PLX4720 with or without IFNβ.

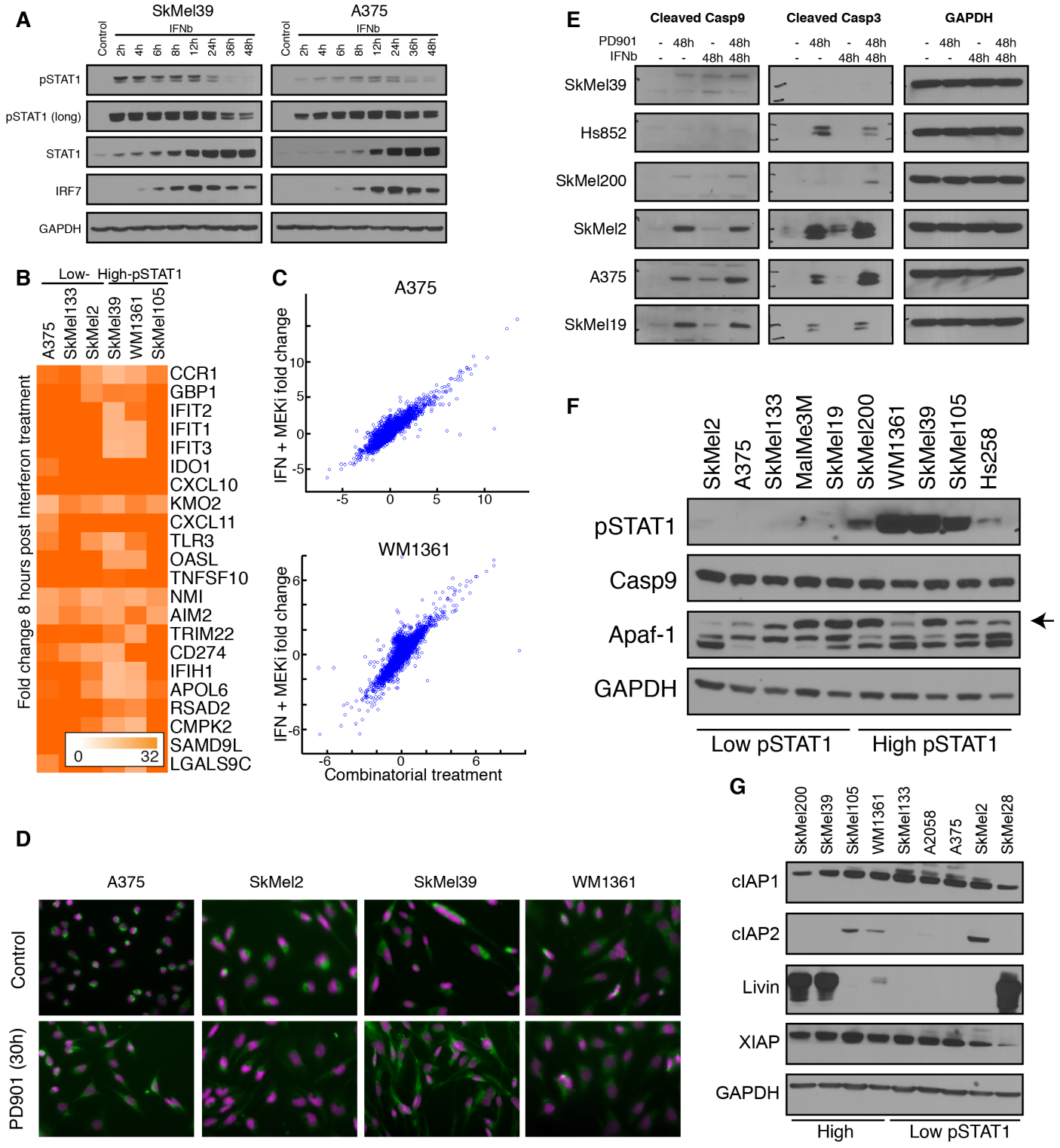

Figure S5 – Related to figure 6 – Identifying the mechanisms underlying response to treatment - **A.** Time course protein levels following treatment with IFNβ of one high

pSTAT1 cell line (SkMel39) and one low (A375). Response amplitude and dynamics is almost identical in the two cell lines. **B.** 22 genes with the highest fold change following IFNβ treatment. The transcriptional response is similar in all cell lines, both with low- and high- basal activation of the pathway. Notably, the fold change of several genes reaches 100 fold, just 8 hours after treatment. **C.** Lack of synergistic and additive effects of MEK inhibition and IFNβ. Scatter plots show the fold change of all genes with a combination of MEK inhibition and IFN (x-axis) and the sum of fold changes with each treatment alone. Significant deviations from the diagonal represent synergism between drugs. Only one gene, CCL4, deviates from the diagonal in all 6 cell lines. **D.** Same as figure 6C, with DAPI staining to confirm nucleus positioning. **E.** Cleaved caspases 9 and 3 following MEK inhibition, IFN treatment, or their combination. This figure includes 4 cell lines that were not part of the original caspase analysis, and were included here to support the association between pSTAT1 levels and activation of the caspase pathway. **F.** Caspase 9 and APAF1 levels (arrow marks APAF1 band) are not correlated with pSTAT1 levels or with cytotoxic response to MEK inhibition. **G.** Levels of known caspase inhibitors are not correlated with the cytotoxic phenotype or pSTAT1 levels.

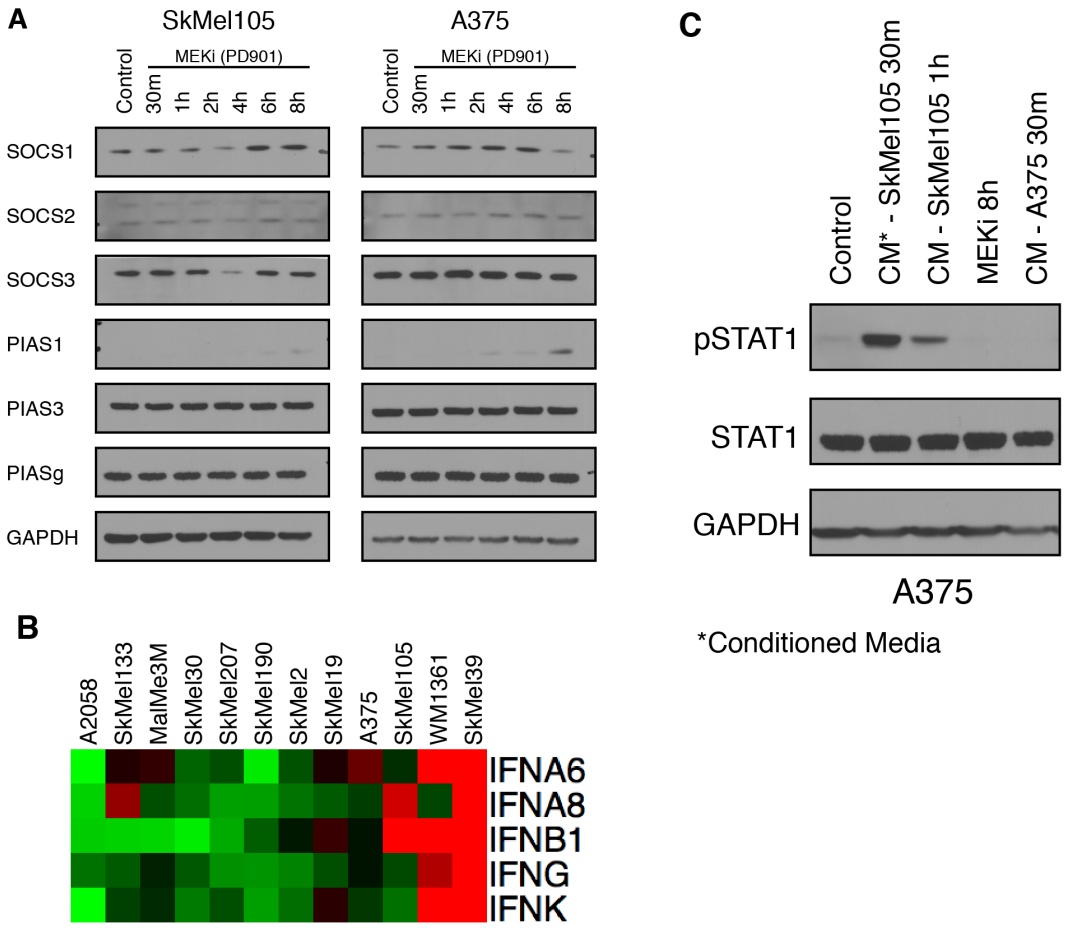

Figure S6 – Related to figure 7 – IFN levels regulated by an autocrine loop and deletion of IFN locus - **A.** Protein levels following MEK inhibition of 6 known inhibitors of the JAK-STAT pathway in two cell lines (SkMel105 - high pSTAT1, A375 – low pSTAT1). Most proteins don't change, although pSTAT1 goes up prior to 8h. Change of PIAS1 is similar in both cell lines. **B.** IFN genes with a significant differential expression between low- and high- pSTAT1 cell lines. IFNA6, IFNA8 and IFNB1 are located in the interferon locus (see figure 7). **C.** Conditioned media experiment shows that SkMel105, a high-pSTAT1 cell line, releases cytokines to the media that lead to the upregulation of pSTAT1. In this experiment, SkMel105 was cultured for 24h, and then the media was transferred to A375, a low-pSTAT1 cell line. Cells were collected 30m and 1h following media transfer. Lanes for MEK inhibition 8h and self-conditioned media (CM-A375) are shown as controls.

Supplementary tables

CTBP2	LDLRAP1
C14orf104	GSK3B
SLC20A2	HERC1
ZNF275	C5orf22
ADSS	TTC15
C8orf55	CREBL2
WDR75	DNAJC3
TRIM65	UBAC1
BAG5	SETD4
SSBP4	BTBD10
LYSMD2	CHD2
TMEM206	ANKRD54
SRXN1	GOT1
ZFAND1	IL16
RCC1	PPM1A
WDR74	CBFA2T2
JMJD4	C19orf12
MTHFD2	KDM4A
WDR89	RCBTB1
NOB1	HOMER3
ANKRD37	SNX30
ZBTB42	WDHD1
ACTR3B	FEM1B
PSMG4	MTMR10
LENG9	AKAP11
NR6A1	
BCORL1	
PAX3	
ABTB1	
ABR	
FNBP1L	
CNPPD1	
ZZZ3	
GNA13	
PEAK1	

Table S1 – List of genes from figure 2A

Gene symbols of the genes from figure 2A. The correlation of these genes with MITF levels is reveled only upon MEK inhibition.

Table S2 – In a separate excel file – List of COSPER modules (Materials and Methods)

Table S2 lists all modules identified by COSPER. Number of genes, and cell lines assigned to each of the contexts are listed for each module.

Antibody	Company	Catalog number
APAF-1	Abcam	Ab32372
Casp 7 (cleaved)	cell signaling	9492
Casp 9 (cleaved)	cell signaling	7237
Caspase 7	cell signaling	9492
Caspase 9	cell signaling	9508
cIAP1	cell signaling	7065
cIAP2	cell signaling	3130
Cytochrome C	abcam	ab110325
GAPDH	cell signaling	5174
IRF1	cell signaling	8478
IRF7	cell signaling	4920
Livin	cell signaling	5471
MITF	abcam	ab12039
pERK1/2	cell signaling	9101
PIAS1	cell signaling	3550
PIAS3	cell signaling	9042
PIASy	cell signaling	4392
pSTAT1 Y701	cell signaling	9167
pSTAT2	cell signaling	4441
pSTAT3 Y705	cell signaling	9138
SOCS1	cell signaling	3950
SOCS2	cell signaling	2779
SOCS3	cell signaling	2932
STAT1	cell signaling	9175
STAT2	cell signaling	4594
STAT3	cell signaling	9139
XIAP	cell signaling	2045

Table S3 – Related to Materials and Methods

List of antibodies used in this study.

Supplementary information

Microarray preprocessing

Samples for microarrays were harvested 8h post treatment. RNA was extracted using a Qiagen RNeasy kit, and labeled using Agilent's one-color labeling protocol. Labeled cRNA was hybridized to Agilent's 8x60 human gene expression arrays (expect for Colo829 and SkMel28 that were added to the panel after the first batch). MEK inhibition and basal state expression levels were measured in biological duplicates. Data normalization is described in supplementary material. Genatomy was used for data visualization and enrichment analysis (Litvin et al., 2009).

Agilent's software was used to assess raw signal intensity. Preprocessing of both the MEKi panel and the IFN experiment was similar. Each of the 3 batches were processed independently - MEKi panel 1, MEKi panel 2 and the IFN panel.

Preprocessing consists of 3 steps – probe filtering, data normalization and probe averaging.

Probe filtering

Log2 values were used from this point on. Probes were filtered based on their values. Probes with low or high levels in more than 20% of samples were removed. This was done to remove noisy and saturated probes. The lower and upper thresholds were different in different batches, depending on labeling, hybridization and scan levels:

Batch	Lower threshold	Upper threshold
MEKi panel 1	6	16
MEKi panel 2	7	18
IFN panel	7	17.5

Additionally, the Agilent probe flags were used to filter probes by a similar method: probes flagged in more than 20% of samples were removed. Flags that were used: will_above_bg, is_saturated, is_feat_non_uniform, is_feat_popn.

A “rescue” step was used to return probes representing genes that no probe was left to represent them. Probes representing the same gene with a high correlation (Pearson >0.75) were rescued. Additionally, probes with high SD (>3) were also rescued.

Data normalization

The 75th percentile of all samples was set to the average 75% by multiplying the values by a constant.

Probe averaging

Probes that measure the level of the same gene were averaged or filtered out.
If the average Pearson correlation between all probes is > .75, probes are averaged. If it is lower, the probe with the lowest correlation is removed. Process repeats till probes are averaged or only two probes are left. If only two probes left and the correlation is low, the probe with the higher raw intensity is chosen.

Merging duplicates

Baseline expression levels are mean-normalized at the gene level. Fold change is calculated against the control (baseline expression) of the cell line. Data from the two MEKi panels are combined at this point by averaging the baseline expression and fold change data.

COSPER - Context-Specific Regulation

COSPER – COntext SPEcific Regulation – is designed to identify genes that are directly regulated by the MAPK pathway (or any other perturbed pathway) in only a subset of cell lines. It is based on the assumption that genes under the direct control of a pathway are correlated before pathway inhibition and show a correlated expression change after pathway inhibition. Since we are looking for genes under the control of the pathway in only a subset of cell lines, we expect expression changes in only these cell lines.

COSPER uses pre-perturbation data to limit the search for genes under direct regulation of the perturbed pathway. After inhibition of a key signaling pathway such as MAPK, cellular events, such as metabolism, cell cycle and apoptosis, lead to expression changes of thousands of genes. Although the expression of those genes changes after MAPK inhibition, they are not *directly* regulated by MAPK. However, genes under the

direct control of MAPK pathway depend on its activation levels both before and after inhibition of the pathway. For example, HEY1 (figure 3A) is under the control of MAPK in only a subset of cell lines. In HEY1 case, it is overexpressed by MAPK in cell lines with high MITF levels. Therefore, only in MITF-high cell lines, HEY1 expression levels decrease after MEK inhibition. Both pre- and post-inhibition expression levels are needed in order to determine this relationship.

COSPER is therefore designed to find genes with context-specific regulation patterns (figure 3B). It is consists of 3 major steps:

1. Gene level – identify binary splits with high scores for both baseline expression and fold change and construct clusters.
2. Merge related clusters – allows removal of spurious correlations and averaging the noise caused due to the small sample size.
3. Add high scoring genes to the remaining clusters

A detailed description of each of the steps follows the section on the NormalGamma score.

NormalGamma score

The algorithm is based on the NormalGamma score (DeGroot, 2004; Segal et al., 2003). The NormalGamma is a Bayesian score that takes variance, mean and number of data points into account. It gives a higher score to a data matrix with low variance.
We use this score since we are looking to reduce the variance of the samples. Our algorithm searches for genes that behave similarly in a subset of samples. For example, we are looking for a subset of samples where a predefined set of genes is up-regulated, compared with the rest of the samples where the genes are not under pathway control. Mathematically, this problem can be viewed as a subset of samples where the data have a lower variance compared with the variance of all samples combined. The NormalGamma score is driven mainly by data variance and is thus suitable for our needs.

The score:

$$N = size(data)$$

$$\beta = \max\left(1, \frac{\lambda(\alpha-2)}{\lambda+1}\right)$$

$$\beta_{plus} = \beta + \frac{Var(data)N}{2} + \frac{N\lambda|data|^2}{2(N+\lambda)}$$

$$\alpha_{plus} = \alpha + \frac{N}{2}$$

$$NormalGamma(data, \lambda, \alpha) = -N * \ln\left(\sqrt{2\pi}\right) + \frac{\ln\left(\frac{\lambda}{\lambda+N}\right)}{2} + \ln\left(\Gamma\left(\alpha_{plus}\right)\right) - \ln\left(\Gamma(\alpha)\right) +$$

$$\alpha \ln(\beta) - \alpha_{plus} \ln\left(\beta_{plus}\right)$$

The score used to assess the quality of the split is:
NormalGamma(right samples) + *NormalGamma*(left samples) - *NormalGamma*(all samples)

Step 1: Creating clusters

First, genes with low fold change and/or low variance in steady state are removed. Genes were considered only if they changed by more than 0.7 fold change (log2 scale) in at least 1 cell line, and at a steady-state expression value of 0.4 in at least 2 samples (to remove genes with extreme outliers in one sample that pass a standard-deviation based threshold). Additionally, all long non-coding RNA transcripts were removed. 5391 genes remain for further analysis.

Then, gene expression is normalized. Basal expression levels of each gene are set to have μ=0 and σ^2=1. Fold change for each gene is standardized only (σ^2=1).

Next, clusters are built bottom-up – genes are assigned to “splits”, and a split with more than one gene assigned to it is considered a cluster. However, in order to filter out spurious associations we only consider clusters with 5 or more genes. All genes are tested across all valid binary splits. A valid split assigns at least 2 samples to each sample group. The test is based on permutations and the NormalGamma score.

A gene is assigned to a split if its NormalGamma scores (as defined in the previous section) in both the baseline expression and fold change are better than 99% of the split

permutations (pvalue<0.01). Additionally, in order to keep the best split-gene pairs only, an additional threshold is used:
NormalGamma (right)+ *NormalGamma* (left)- *NormalGamma*(all samples)>0

To determine whether clusters with more than 5 genes can be constructed by chance. We permuted the samples in the fold change expression data and performed this step on the permutated data. No clusters with 5 or more genes were constructed. Hence we believe the resulting clusters represent biological phenomenon.

Step 2: Merging clusters

A gene assigned to a split is very likely to be assigned to similar splits. A similar split might have one or more samples switching "sides" (figure 4A). Each split has 13 similar splits with a distance=1, where one sample has switched sides, and 91 splits with distance=2.
The NormalGamma score is not strong enough to discriminate between the "true" split and neighboring splits, since the distribution of scores is very tight. However, we can assume that a gene is more likely to be assigned to the real biological split, and less likely to be associated with a split with a distance>0 from the real split. We also work under the assumption that a true biological "context" is likely to influence many genes, and therefore larger clusters are more biologically relevant.
We use these two assumptions in order to identify the real gene-split associations and remove irrelevant clusters.

The cluster merging algorithm is a iterative process. Each cycle identifies the largest cluster, its genes are removed from all its neighboring clusters, and the process iterates till no more clusters can be identified.

The steps are:

1. Each cluster is scored based on its overlap with its neighbors:

$$Score(cluster_x) = \sum_{i \text{ where } Distance(Split_X, Split_i) \leq d} \#(Genes_{Cluster_x} \cap Genes_{Cluster_i})$$

   we used d=2.

2. We then choose the largest cluster, and remove its genes from all clusters with a distance<=d.

To save computing time, only clusters that enter the algorithm with 5 or more genes are allowed to be selected.

Step 3: Adding genes to remaining clusters

In the last step, after filtering most clusters out, we allow genes from neighboring clusters to be added back to clusters. We found this step to be necessary due to the small sample size, the overall small distance between clusters, the relatively high noise of gene expression data, and the inability of the *NormalGamma* score to discriminate between similar splits.
Genes belonging to clusters in a distance<=d of a specific cluster, and with a pvalue<0.01 are added to this cluster.

*Code available on Pe'er lab's website (http://www.c2b2.columbia.edu/danapeerlab/html/).

Perturbation reveals patterns hidden in pre-perturbation data

To identify genes that are correlated only post- but not pre- perturbation we used a method similar to step 1 in COSPER. Specifically, we searched for clusters that show the behavior depicted in figure 2B, by associating genes to clusters only if they have a good score in post-perturbation data, but a bad score in steady state data.

We used stringent thresholds to define "good" and "bad" scores. The good score was defined as a permutation-based NormalGamma score < 0.01, and a bad score was with a permutation p-value > 0.5. Additionally, we require that a gene will be associated only if the post-perturbation NormalGamma score will demonstrate:
NormalGamma (right)+ *NormalGamma* (left)- *NormalGamma*(all samples)>0
While the pre-perturbation score will be:

NormalGamma (right)+ *NormalGamma* (left)- *NormalGamma*(all samples)<0

To remove spurious associations, we only considered clusters with > 20 genes. Overall, 3941 genes were associated with one or more clusters. As an example to this behavior, we show one such cluster in figure 2A.

COSPER results on steady-state or post-inhibition data alone

Combining pre- and post-inhibition data facilitates the identification of context-specific regulation and differential activation of pathways, while pre-inhibition data or steady state data alone fall short due to lower specificity and sensitivity.

We ran COSPER on each data set alone (pre or post inhibition). The number of modules increases dramatically, to 2684 with steady state data, and 1524 with post-inhibition data, compared with only 70 when using both data sets. Specificity is lost and those numbers make it much harder to analyze and interpret the results, while also increase the statistical burden for any post-analysis statistical tests.

Additionally, each cluster becomes much larger and less specific to MAPK targets. For example, STAT3 module contains 740 genes, compared with 28 genes using both datasets. While the later cluster is enriched for STAT3-related terms, the larger pre-inhibition cluster is enriched for MITF related annotations, although the one group of samples contains both MITF-positive (3) and MITF-negative (8) cell lines. The influence of MITF in melanoma is so strong (Principal component 1 is correlated with MITF and explain 30% of the variance), that by using only steady-state data all other signals become undetectable. Overall, the modules when running with steady state data alone are much larger, containing on average 194 genes compared with 33 when using the two datasets. This hampers power of many analysis tools, including LitVAn and gene set enrichment.

COSPER results on post-inhibition data alone are even less informative, with enrichments and biological coherence for both the STAT3 and STAT1 modules completely missing and we no longer have tight modules that can narrow down individual pathways. Instead we see general processes expected from inhibition of a

key oncogenic pathway, such as cell cycle regulation, changes in metabolism, signal transduction, etc.

The combination of pre- and post-inhibition data, therefore, provides specificity and limits the cluster genes to only genes directly regulated by MAPK, while also provides the context of regulation.

Comparison of BRAF and MEK inhibition - PLX4720 vs. PD901

We used PD901 to inhibit the MAPK pathway, and not the more clinically used PLX4720 BRAF-V600E inhibitor to allow a direct comparison of BRAF and NRAS mutant cell lines. To ensure the short-term drug effects are similar, we compared the transcriptional response of MalMe3M, a BRAF-V600E cell line, following PD901 or PLX4720 treatment. We assessed expression fold change at 1 hour, 2, 4, and 8 hours following treatment using Illumina HumanHT-12 microarrays.

Preprocessing

Illumina's probe pvalues were used to filter out probes. Probes with p-value>0.05 in more than half of the samples were removed. Then microarrays were normalized according to their 75% percentile values. The 2 control array were averaged, and treated samples were compared to the averaged control to assess fold change.

Results

MEKi and BRAFi are remarkably the same at all time points. Although some probes were noisy, resulting in minor difference between treatments, no gene had a difference greater than 0.5 fold (on a log2 scale) between treatments at all time points. Only 6 probes, out of 16000, had a difference of more than 1 fold at 8 hour time point (figure S1B). None of them had such difference at 4 hours, suggesting that the difference arises from measurement noise.

We conclude that there is no difference in the short-time transcriptional response between treatments in this cell lines.

Comparison of the response to MEK inhibition between known genetic contexts

Both inactivation of PTEN and the type of MAPK activation (BRAF or NRAS) have been previously associated with the response to MAPK pathway inhibition. We examined whether these mutations are correlated with the transcriptional response to MEK inhibition or the basal expression levels prior to MEK inhibition.

We used t-test to compare the expression levels between BRAF- and NRAS mutant cell lines (figure S2A), and between PTEN-null and PTEN-wild type cell lines (figure S2B). In both cases we found that no genes are associated with those genetic contexts (FDR q-value < 0.05), either before of after pathway inhibition.

PD901 and IFNβ microarray results

Data Preprocessing

Six cell lines were chosen for analysis. 3 are low-pSTAT1 – A375, SkMel133 and SkMel2, and 3 high-pSTAT1 – SkMel105, SkMel39 and WM1361. They were treated with 50nM PD901, 1000U/mL IFNβ or their combination. Samples were collected 8 hours after treatment, control samples were collected at 0h. RNA extraction, labeling and hybridization were conducted as described under methods. Agilent human 8x60 gene expression arrays were used.

Raw data normalization and filtering were conducted as described above, with a low threshold of 7, and an upper threshold of 17.5.

IFN response in high- vs. low- pSTAT1 cell lines

The IFN response includes dozens of genes with a dramatic induction in gene expression, of up to 500 fold, in all 6 cell lines (figure S5B).

There is, however, a difference in the extent of change in high- vs. low- pSTAT1 cell lines, that can be attributed to the different basal expression level of those genes (data not shown). The maximum level of expression seems to be similar in all cell lines, but high pSTAT1 cell lines have a higher basal activity and therefore the fold change is lower.

In order to compare the activation of the pathway between the two cell line groups, it is better to use the final expression level, i.e. the basal expression+fold change. However, such comparison reveals the expression of no genes is statistically significant different between high- and low-pSTAT1 cell lines (using t-test and FDR correction).

We therefore determine that there is no difference in the response to IFNβ between high- and low-pSTAT1 cell lines.

Combinatorial treatment and synergy

To test whether the MEK inhibition and IFNβ synergize at the level of gene expression, we compared the fold change of the dual treatment with that of MEKi+IFNβ as single agents. Over all, those responses are very similar (figure S5C).

If no synergy exists, the values of Both-(MEKi+IFNβ) should be close to 0. Only one gene significantly deviates from 0 in all 6 cell lines. The gene is CCL4, and it is induced both by MEKi and IFNβ treatment as single agents, but a combinatorial treatment isn't additive.

We couldn't identify any other genes that show a synergetic response in all 6 cell lines, or separately in low- or high-pSTAT1 lines (we defined synergy is the equation above >1 or <-1).

MITF binding site analysis

To assess frequency of MITF binding site in gene promoters we used the motif CACATG, known to be a target sequence of MITF. Gene promoters were defined as 5000bp upstream of their transcription start site, or up to the closest upstream gene, whichever is shorter. For each gene, number of binding motif in its promoter sequence was noted.

To assess the significance of number of motif occurrences, we used the binomial distribution. Since the MITF-M and MITF-expression clusters are similar and share genes, for the purpose of this analysis genes were assigned to only one of the clusters based on their NormalGamma score. For each one of the two clusters, MITF-M and MITF-expression, we counted total number of motif occurrences in all the cluster genes. For simplicity, the expected probability of the motif to randomly appear in a DNA sequence is $2*1/4^6$ (6 is the length of the motif, and 2 represent the two strands).

The pvalue of X occurrences is the probability of randomly observing X or more occurrences in a random sequence, or 1-BINOMIAL_CDF(X, N, p), where N is total sequence length and p is $2/4^6$.

For MITF-M cluster, the total promoter sequence is 120735bp, with 83 motif occurrences (59 expected). For MITF-expression cluster, the total promoter sequence is 183399bp, with 86 occurrences (89 expected).

Cytochrome C release

Protocol for Cytochrome C release is taken, as is, from Majewski et al 2004. It is brought here for convenience:

Lysis buffer: 20 mM Hepes-KOH, [pH 7.5], 210 mM sucrose, and 70 mM mannitol; 1.5 mM MgCl2, 10 mM KCl2, protease inhibitor, and 1 mg digitonin/1mL lysis buffer.

Cells are trypsinized, collected and spun down in 4C. They are then washed with PBS and spun down again. It is critical that cell pellets will be lysed immediately without freezing.

Cells are gently suspended, without vortexing, in lysis buffer. Roughly double the cell pellet volume is used. They are incubated in 25C for 3-10min, depending all cell line. Spun down at 4C for 20 minutes at highest speed. Supernatant contains cytoplasmic fraction.

Protein concentration was assessed using BCA.

Fluorescent Microscopy

Cells were plated onto Corning BioCoat Poly-D-Lysine glass 8-well culture slide (Corning 354632) at a density of 15,000 to 40,000 cells/well and allowed to attach to the surface for 24 hours. Cells were then treated with 50 nM PD0325901, and the same volume of DMSO was added to controls at the time of treatment.

CytoC released was measured 30 hours after treatment. Cells were washed 1X with PBS, fixed with 4% PFA in PBS for 10 min at room temperature, and washed 2X with PBS (5 min / wash). Cells were then blocked and permeabilized in 5% BSA/0.3% TX-100 in PBS for 1 hr at room temperature.

Cells were incubated with Anti-Cytochrome C antibody (Abcam ab110325) at 1 µg/mL in 1% BSA/0.1% Tween-20 in PBS overnight at 4 °C, when washed 3X with 1% BSA/0.1% Tween-20 in PBS (5 min / wash), and then incubated with Alexa Fluor 488 Goat Anti-Mouse IgG2a (γ2a) (Molecular Probes A-21131) at 1 µg/mL in 1% BSA/0.1% Tween-20

in PBS for 45 min in the dark at room temperature. Cells were washed 3X with 1% BSA/0.1% Tween-20 in PBS (5 min / wash).

Cells then were counterstained with NucBlue Fixed Cell ReadyProbes Reagent (Molecular Probes R37606) for 10 min, and washed in 2X with PBS (5 min / wash).

Slides were mounted with Fluoro-Gel with Tris Buffer (Electron Microscopy Sciences17985-10), and images were acquired using an inverted microscope (Nikon Eclipse TE2000-E) equiped with a 40X lens and illuminated with a mercury vapor short arc lamp (Olympus X-Ctie 120PC).

References

DeGroot, M.H. (2004). Optimal statistical decisions, Wiley classics library edn (Hoboken, N.J.: Wiley-Interscience).

Litvin, O., Causton, H.C., Chen, B.J., and Pe'er, D. (2009). Modularity and interactions in the genetics of gene expression. Proceedings of the National Academy of Sciences of the United States of America *106*, 6441-6446.

Segal, E., Shapira, M., Regev, A., Pe'er, D., Botstein, D., Koller, D., and Friedman, N. (2003). Module networks: identifying regulatory modules and their condition-specific regulators from gene expression data. Nature genetics *34*, 166-176.